NUCL SCI TECH (2018) 29:87
https://doi.org/10.1007/s41365-018-0424-y

Electron-beam radiation effects on the structure and properties of polypropylene at low dose rates

Heng-Ti Wang[1,2] · Hai-Qing Jiang[1] · Rong-Fang Shen[1] · Xiao-Jun Ding[1] · Cong Zhang[1] · Lin-Fan Li[1] · Jing-Ye Li[1]

Received: 14 December 2017 / Revised: 14 February 2018 / Accepted: 27 February 2018 / Published online: 30 April 2018

Abstract While the high-energy radiation effects on polypropylene, which are crucial for the cable industry for nuclear power plants, have been thoroughly studied, the property changes of PP at low-dose-rate electron-beam irradiation are far from elucidated. Herein, the influence of electron-beam irradiation on the structure and properties of PP was examined. The static EB irradiation conditions were 1.2 MeV at a low dose rate of 20 kGy/h to achieve absorbed doses ranging from 45, to 60, 100, and 200 kGy. The molecular structure was first evaluated by measuring the carboxyl index and the relative radical concentrations via Fourier transform infrared spectroscopy and electron spin resonance, respectively. Mechanical, differential scanning colorimetric, and rheological tests were carried out to further investigate the changes in the properties (tensile, crystalizing, and viscoelastic properties) of irradiated PP, which showed good agreement with the structural analysis results. We found that radio-oxidative degradation (chain scission) was predominant, which can be due to the low dose rate facilitating oxygen diffusion into the PP matrix during electron-beam irradiation.

Keywords Electron beam · Radiation effect · Low dose rate · Polypropylene

1 Introduction

Nuclear cables are regarded as vital components for nuclear power plant (NPP) control systems and instrumentation [1]. Safety-related cables must be qualified to be functional not only under special NPP service conditions over their lifetime, but also against severe design-basis event (DBE) conditions [2, 3]. Polyolefin is the base material most used in the cable industry. Thus, the effects of high-energy radiation on polyolefin have attracted attention from the academic and industrial fields, especially after the Fukushima Daiichi nuclear event [4–6]. Generally, irradiation (e.g., γ-rays, β-rays, X-rays, electron beams, or ion beams) of polyolefin leads to the formation of free radicals [7]. Polyolefin then undergoes grafting of long chain branches (LCB) [8], chain scissions [9], and cross-linking [10] reactions by virtue of the exited species. Previous studies showed that the ultimate radiation effects on polyolefin are mainly related to various factors including molecular structure [11], atmosphere [12], and radiation conditions (type of radiation, dose rate, and absorbed dose) [13].

Polypropylene (PP) is one of the most used polyolefin materials in the nuclear cable industry because of its moisture [14] and chemical resistance [15], low density, and relatively low cost [16]. Compared with low-density polyethylene (LDPE), PP displays better rigidity and

This work was supported by the "Strategic Priority Research Program" of the Chinese Academy of Science (No. XDA02040300) and the National Natural Science Foundation of China (No. 11575277).

✉ Lin-Fan Li
lilinfan@sinap.ac.cn

✉ Jing-Ye Li
lijingye@sinap.ac.cn

[1] Shanghai Institute of Applied Physics, Chinese Academy of Sciences, Shanghai 201800, China

[2] University of Chinese Academy of Sciences, Beijing 100049, China

thermo-mechanical resistance [17]. However, PP is more susceptible to degradation under irradiation due to the tertiary carbon atom at every monomer unit [18]. It has been verified that β-chain scission is predominant when PP is exposed to high-energy irradiation [19]. There are many reports available on the γ-ray radiation effects on PP to understand the radiation-induced degradation mechanisms of PP. Hnát et al. [20] have reported that β-rays were predominant within the radiation source (involving approximately 80% soft β-ray irradiation) during DBEs. Moreover, the requirement of low-dose-rate β-ray irradiation tests has been put forward according to third-generation NPP design, such as AP1000. AP1000 regulations, developed in US-based company Westinghouse, point out that investigations on β-ray irradiation should be carried out in nuclear security systems for reducing the probability of occurrence of human error. Additionally, AP1000 regulations recommend using 1.2 MeV electron beams (EB) at a dose rate of 20 kGy/h to simulate β-ray irradiation during the cable material tests. Abraham et al. [21] have investigated EB irradiation at 3.5 MeV with high dose rates, and their results indicated that the degradation of PP was predominant and increased with increased absorbed doses. Recently, Jahani et al. [22] reported that the kinetics of PP degradation reactions were determined by its chemical structure and irradiation conditions under 10 MeV EBs.

These results pose several questions. The information on EB radiation effects at low dose rates is not available in the literature, because EB irradiation is usually performed at high dose rates during polymer processing. It is imperative to understand EB irradiation effects with low dose rates on PP, from the point of view of the NPP cable industry.

The main objective in this paper is to investigate the radiation mechanisms of PP under 1.2 MeV static EB irradiation with a dose rate of 20 kGy/h. For this purpose, atactic PP without antioxidants was irradiated to achieve absorbed doses of 0, 45, 60, 100, and 200 kGy at an ambient temperature of 25 °C in air. Changes in the molecular structure of the irradiated PP were measured in terms of the carboxyl index (CI) and the relative radical concentration (C_{Radical}) using Fourier transform infrared spectroscopy (FTIR) and electron spin resonance (ESR) measurements, respectively. Mechanical, differential scanning calorimetric (DSC), and rheological tests were carried out to further investigate the changes in the properties (tensile, crystalizing, and viscoelastic performance) of irradiated PP, as a function of the absorbed dose. From these characterizations, it is possible to get the quantitative information on the changes in the properties of PP by EB irradiation required by AP1000 regulations.

2 Experimental section

2.1 Materials

The PP used is a homopolymer of atactic configuration (Sumitomo Co., Japan) with the trade name of AH561. The density (ρ) and melt flow index (MFI) of this PP were 0.90 g cm^3 and 0.3 g/min (ASTM D-1238), respectively. The melting point (T_m), crystallinity (X_c), and crystallization temperature (T_c) of PP were measured to be 163.2 °C, 38.1%, and 113.3 °C, respectively, obtained via thermal analysis.

2.2 EB irradiation

PP sheets (10 × 10 × 1 mm^3) were irradiated statically with 1.2 MeV at a dose rate of 20 kGy/h to achieve absorbed doses of 0, 45, 60, 100, and 200 kGy. All the irradiated samples were immediately preserved in a nitrogen atmosphere at 10 °C until further characterizations.

2.3 Characterization

2.3.1 Molecular structure of the irradiated PP

ESR measurements (FA200, JEOL, Japan) were taken immediately after irradiation. The spectroscopic parameters are listed as follows: microwave frequency of 9078.29 MHz, central magnetic field of 325.41 mT, and modulation frequency of 100.0 kHz. The double integration method was utilized to calculate C_{Radical} values.

FTIR measurements (VERTEX 70 V, Bruker, Germany) were taken in transmittance mode. FTIR spectra were recorded with 64 scans at a resolution of 1 cm^{-1}. CI values were calculated by Eq. (1) from FTIR spectra,

$$\text{CI} = \frac{I_{1170\,\text{cm}^{-1}}}{I_{1720\,\text{cm}^{-1}}}. \quad (1)$$

Here $I_{1170\,\text{cm}^{-1}}$ and $I_{1720\,\text{cm}^{-1}}$ refer to the integral area of the characteristic peak of methyl and carbonyl groups, respectively.

2.3.2 Properties of the irradiated PP

Tensile tests were carried out at 25 °C using an universal material testing system (model 5966, Instron, Germany) to investigate PP's mechanical properties. Samples were punched into a dumbbell shape (180.53 mm^3), and the cross-speed was 10 mm/min.

DSC measurements (Q2000, TA, USA) were taken for thermal analysis. Tests were conducted at a heating rate of 10 °C/min from − 50 to 200 °C. All specimens were tested in a continuous high-purity nitrogen atmosphere.

Rheological behaviors were determined using a rotating rheometer (MCR301, Anton Paar GmbH, Austria) with a parallel-plate model (with a gap of 1 mm and a diameter of 25 mm). Amplitude sweeping was first conducted at 200 °C with a fixed frequency of 1 Hz. The strain amplitude (γ) ranged from 0.01 to 1000%. A linear viscoelastic (LVE) region was determined ($\gamma_{LVE} = 0.1 - 100\%$) based on the amplitude sweeping tests. Small amplitude oscillation shear (SAOS) tests were then carried out with a γ of 5% at 200 °C in the frequency range of 0.01 to 500 rad/s. Cole–Cole plots, which are a representative criterion, were plotted according to the SAOS data. For better understanding, weighted relaxation spectra and molecular weight distribution curves were deduced via the edge preserving regulation [23] and the Laplace transform [24] methods using the Rheoplus software.

3 Results and discussion

3.1 Effects on the molecular structure of PP

In order to clarify the chemical reactions during 1.2 MeV EB irradiation at 20 kGy/h, the ESR and FTIR spectra of pristine and irradiated PP are illustrated in Fig. 1.

ESR measurements were a useful tool for analyzing the presence and type of free radicals of the radiated specimens. Figure 1a shows the ESR plots of the irradiated PP for various absorbed doses, namely 45, 60, 100, and 200 kGy, which were measured immediately after irradiation. It is clear that the intensity of the ESR signal increased as the absorbed dose increased. The $C_{Radical}$ values were determined from the ESR curves, as listed in Table 1 and plotted in Fig. 1c. The variation of the $C_{Radical}$ values agreed well with the plot presented in Fig. 1a, increasing from 5.65×10^{14} spin/g (45 kGy) to 6.65×10^{14} spin/g (60 kGy), 12.9×10^{14} spin/g (100 kGy), and 17.8×10^{14} spin/g (200 kGy). $C_{Radical}$ values after 144 h were also calculated and are shown in Fig. 1c (details in Table 1). These suggest that the concentration of radicals in this system levelled off and decayed within 6 days. Moreover, multi-peaks with complex shapes were observed for all specimens. We determined that high-energy irradiation of PP initially produces alkyl radicals [25]. Due to the existence of oxygen (O_2), alkyl reacted with O_2 to form peroxide radicals and even ROOH via hydrogen abstraction reactions [25, 26]. Mowery et al. [26] indicated that mainly tertiary radicals formed upon irradiation of PP. The results indicated the coexistence of tertiary alkyl and peroxide radicals when PP was irradiated.

Figure 1b displays the expanded FTIR spectra of the pristine and irradiated PP. The recorded curves were normalized for better comparison, based on the characteristic peak at 1170 cm^{-1} (stretching of –C–CH_3 on the PP chain). The largest structural variation occurred at 1720 cm^{-1}, corresponding to the stretching vibration of carbonyl groups, which were not found for the pristine PP. As the absorbed dose increased, the intensity of the carbonyl band increased proportionally. The CI*s* of the irradiated specimens were calculated from the FTIR spectra using Eq. (1), and we found that the CI values showed a positive correlation with the absorbed doses, as illustrated in Fig. 1c and listed in Table 1. These results are consistent with the work of Sevil et al. [27], which involved γ-irradiated isotactic polypropylene. Khang et al. [28] and Fintzou et al. [29] also observed similar results in previous studies, where they claimed that the radiation-induced oxidation and that it was the reason for the increase in the CI values. It is possible that the EB irradiation in air allowed for the formation of oxidized groups from chain scission reactions as a result of the presence of oxygen. Besides, slightly increased intensities of weak signals at 1044 and 943 cm^{-1} were observed. These peaks were attributed to the stretching vibration of C–O–C and terminal C=C bonds on the PP chains [30]. This can be explained by the chain scission reaction of PP macro-

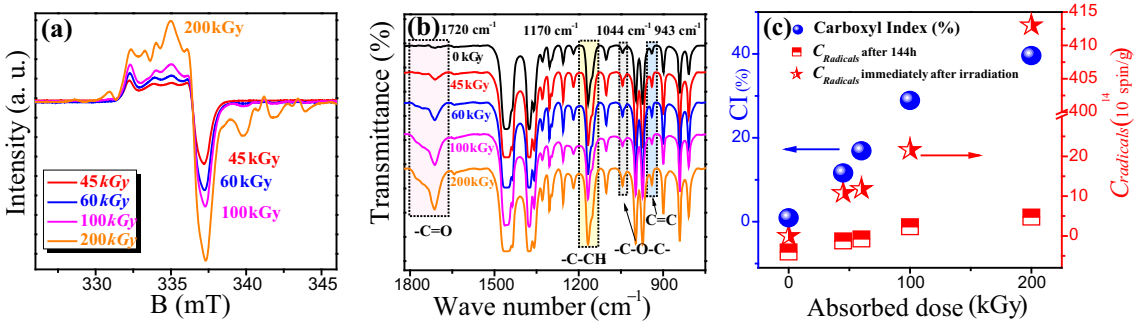

Fig. 1 (Color online) **a** ESR spectra and **b** FTIR spectra of pristine and irradiated PP; **c** The CI and relative radical concentrations ($C_{Radical}$: immediately and after 144 h) of the irradiated PP specimens as a function of absorbed dose, ranging from 45 to 200 kGy

Table 1 Numerical data for $C_{Radical}$ and CI and the mechanical properties of 1.2-MeV-EB-irradiated PP at a low dose rate (20 kGy/h)

Absorbed dose (kGy)	$C^{a}_{Radical,\ 3\ h}$ (10^{14} spin/g)	$C^{a}_{Radical,\ 144\ h}$ (10^{14} spin/g)	CI[b] (%)	Yielding strength (MPa)	Elongation at break (%)	Young's modulus (MPa)
0	–	–	0.9	34.3 ± 2.8	832.9 ± 18.5	808.9 ± 1.6
45	10.8	5.65	11.6	33.9 ± 1.9	8.5 ± 3.2	1008.7 ± 3.5
60	11.8	6.65	16.9	31.3 ± 1.6	5.7 ± 3.6	1078.9 ± 2.6
100	21.6	12.9	28.9	21.8 ± 1.8	3.3 ± 1.8	1012.5 ± 2.3
200	413	17.8	39.6	12.4 ± 0.1	1.9 ± 0.1	1132.9 ± 1.8

[a]Sample dissolved completely in o-xylene

[b]$C_{Radical}$ calculated from the ESR data of LDPE sheets for various absorbed doses, measured immediately after the irradiation process.

[c]The CI*s* were calculated from the FTIR spectra as $CI = \frac{I_{1170\,cm^{-1}}}{I_{1720\,cm^{-1}}}$, where $I_{1170\,cm^{-1}}$ and $I_{1720\,cm^{-1}}$ refer to the integral area of the characteristic peaks of methyl and carbonyl groups, respectively

radicals under irradiation. We acknowledged that the termination mechanisms of free radicals, such as branching (grafts formation), cross-linking, and degradation (formation of oxidized products), depend strongly on molecular structure. Compared with LDPE, PP is a more complicated system involving primary, secondary, and tertiary carbons. A previous study confirmed that the majority of the oxidation-functionalized groups form on the tertiary carbons of PP because the intermediate tertiary radicals are more stable [26]. These intermediate radicals can further react to develop tertiary oxidized products, which is in good agreement with our FTIR observations. We determined that oxidative degradation was predominant for PP irradiated by 1.2 MeV EBs at 20 kGy/h.

3.2 Effects on the property of PP

In order to verify the proposed oxidative degradation of PP under low-dose-rate EB irradiation, the changes in the properties in dependence of the absorbed dose were taken into account. Variations on the mechanical, thermal, and rheological performances of the irradiated PP are discussed in this section.

3.2.1 Mechanical properties

Figure 2a, b shows the stress–strain curves of PP as a function of the absorbed dos. The pristine PP showed typical ductile tensile behaviors, while all of the irradiated PP specimens became brittle, as shown in Fig. 2a. Moreover, Fig. 2c indicates that the values of elongation at break decreased as the absorbed dose increased. The data on tensile strength and Young's modulus are also shown in Fig. 2c (and are detailed in Table 1). While the Young's modulus values remained constant, both the values of tensile strength and elongation at break decreased as the absorbed dose increased. This trend is consistent with previous observations that reported that the loss of mechanical properties was closely related to oxidative chain scission of polymers upon ionizing radiation [31]. We can speculate that it was the radiation-induced oxidative degradation that led to the deterioration of the mechanical properties.

3.2.2 Thermal behaviors

The shape of the calorimetric curves can provide effective information on the structural characteristics and thermal history of irradiated samples. DSC thermograms of the pristine and irradiated PP are illustrated in Fig. 3. Detailed thermal parameters are listed in Table 2.

Figure 3a shows the recorded first heating curves. Pristine PP exhibited only one melting peak at 165.3 °C, indicating that PP is characterized by one crystalline form [19, 32]. After irradiation, the melting peak of PP shifted to a lower temperature with a shoulder peak. Besides, both melting peak temperatures and the melting enthalpy (Table 2) decreased as the absorbed dose increased. Similar trends were found for X_{c1} values. Because the crystal form of the irradiated PP was unchanged, as determined from the Raman spectra (Fig. 3d, e) and X-ray diffraction results (Fig. 3f), this implies that PP became more amorphous after irradiation. These results are in good agreement with previous works, where a decreasing T_m for PP under increasing doses of γ-ray irradiation was observed [33]. Yagouni et al. [34] reported that irradiation on PP causes molecular variations that shorten the polymer chains and thus reduce the T_m values as a function of the absorbed dose.

The cooling thermograms are shown in Fig. 3b. We found that the crystalizing temperature (T_c) of the irradiated PP was always higher than that of pristine PP (113.3 °C), while the T_c values decreased as the absorbed dose increased from 45 (115.3 °C), to 60 (115.0 °C), 100

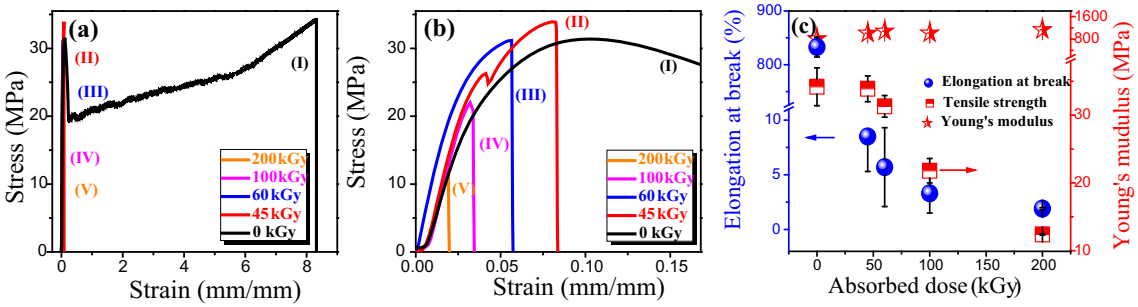

Fig. 2 (Color online) Mechanical properties of the irradiated PP for various absorbed doses: **a**, **b** Strain–stress curves; **c** Young's modulus, tensile strength, and elongation at break

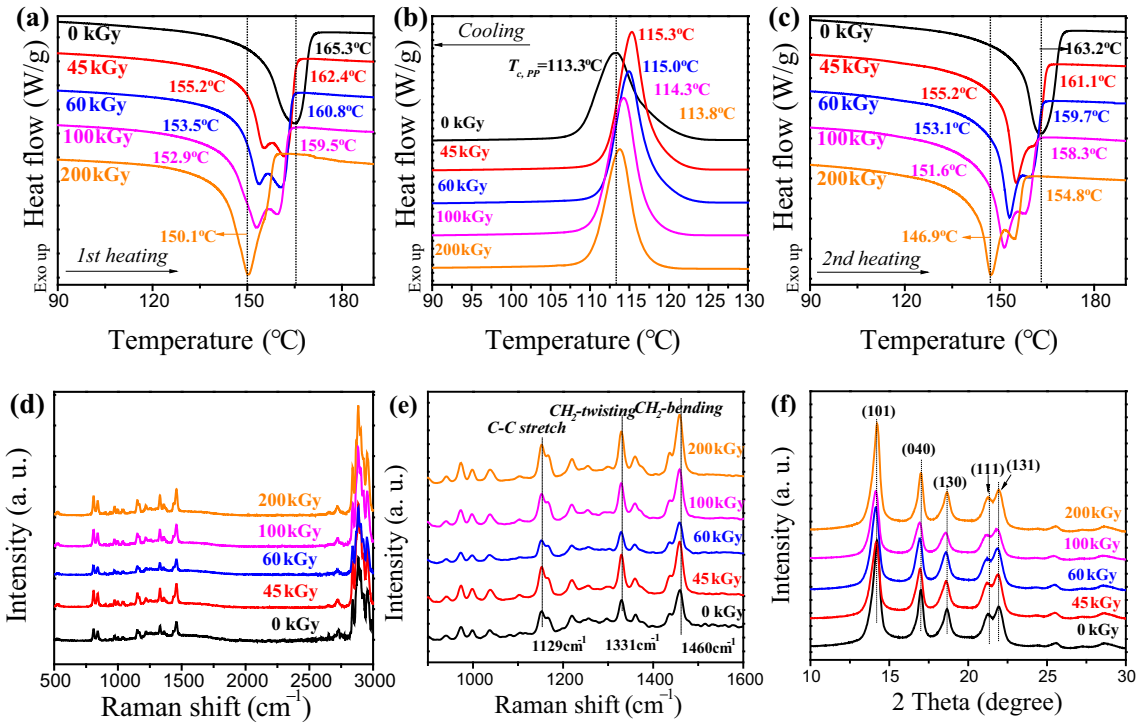

Fig. 3 (Color online) DSC thermograms: **a** first heating, **b** first cooling, and **c** second heating curves; **d**, **e** Raman spectra and **f** X-ray diffraction (XRD) of the pristine and irradiated PP for various absorbed doses

(114.3 °C), and 200 kGy (113.8 °C). These results suggest that the occurrence of the degradation on the PP chains somewhat reduced the number and size of the crystal domains. Because the major radiation effect on PP was degradation, PP with reduced molecular weight was formed as a function of the absorbed dose. In consequence, several spherulites of smaller dimensions were formed, which explains the reduced T_c values as well as the shoulder melting peak for increased absorbed doses.

A second heating procedure was conducted to investigate the melting and enthalpy variations of the irradiated PP, as shown in Fig. 3c. Both the melting point and enthalpy values in the second scan slightly decreased, compared with their first scan counterparts (Table 2). This can be attributed to re-degradation reactions during the first heating process by virtue of "frozen radicals" within crystalline regions [8, 15].

Based on the DSC results, the reduction in T_m can be attributed to accelerated chain scission reactions during irradiation. These reactions reduce the amount of tie molecules in the amorphous regions and, thus, weaken the laminar concentrations [14, 35].

3.2.3 *Rheological properties*

The melt rheological behaviors were very sensitive for assessing the changes in the molecular structures, such as chain scission, branching, and cross-linking [14].

Table 2 Thermal parameters of the pristine and irradiated PP obtained from the DSC measurements

Absorbed dose (kGy)	T_c^a (°C)	$T_{m,first}^b$ (°C)	$T_{m,second}^c$ (°C)	ΔH_c^d (J/g)	$\Delta H_{m,first}^e$ (J/g)	$\Delta H_{m,second}^f$ (J/g)	X_{c1}^g (%)	X_{c2}^h (%)
0	113.3	165.3	163.2	86.3	79.4	79.6	38.0	38.1
45	115.3	155.2, 162.4	155.2, 161.1	89.6	91.6	89.2	43.8	42.7
60	115.0	153.5, 160.8	153.1, 159.7	86.4	90.2	88.6	43.2	42.4
100	114.3	152.9, 159.5	151.6, 158.3	82.3	92.6	81.0	44.3	38.8
200	113.8	150.1	146.9, 154.8	76.2	88.5	74.3	42.3	35.6

[a]T_c: peak temperature during the cooling scanning in the DSC data

[b]$T_{m,first}$: peak temperature during the first heating scanning in the DSC data

[c]$T_{m,second}$: peak temperature during the second heating scanning in the DSC data

[d]ΔH_c: enthalpy of crystallization from the cooling scanning

[e]$\Delta H_{m,first}$: enthalpy of fusion from the first heating scanning

[f]$\Delta H_{m,second}$: enthalpy of fusion from the second heating scanning

[g]X_{c1} and [h]X_{c2}: PP crystallinity calculated from $\Delta H_{m,first}$ and $\Delta H_{m,second}$ using 209 J/g of $\Delta H°_m$ for 100% crystalline PP, respectively

Amplitude sweeping tests were first carried out, as shown in Fig. 4a. We observed that the values of the complex modulus ($|G^*_{(\gamma)}|$) decreased over the whole strain amplitude (γ) range, as a function of the absorbed dose. This was consistent with previous results indicating that oxidative degradation was predominant when PP was irradiated by 1.2 MeV EBs at low dose rates. Based on these results, the critical γ value within the LVE region of all specimens was determined as 5% and was used for further investigation.

Figure 4b, c shows the complex viscosity ($|\eta^*_{(\omega)}|$) and the damping factor ($\tan \delta_{(\omega)}$) of the samples against angular frequency (ω), measured through SAOS tests. More detailed information on the linear viscoelastic behaviors, such as the $G'_{(\omega)}$ and $G''_{(\omega)}$ values of the irradiated PP, are shown in Fig. 4d, e. Pristine PP exhibited a Newtonian behavior up to an ω of 0.6 rad/s. Upon irradiation, $|\eta^*_{(\omega)}|$ decreased severely within the full range of ω measured. Moreover, the reduction rate of $|\eta^*_{(\omega)}|$ was proportional to the absorbed dose. Similar trends were found, as shown in

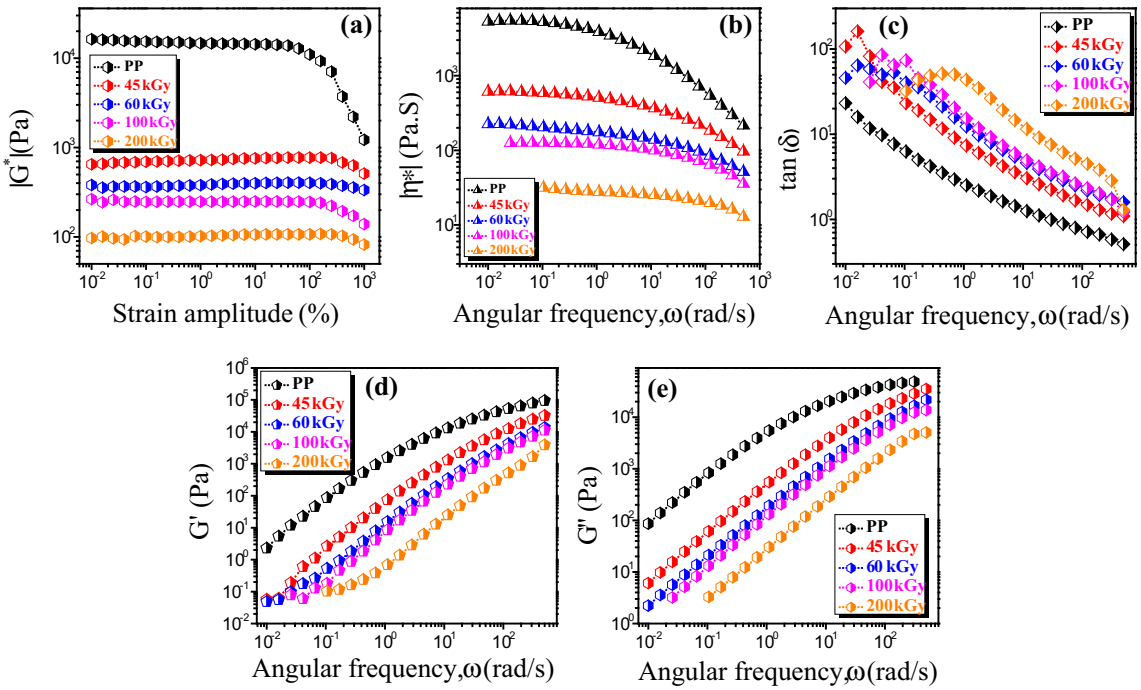

Fig. 4 (Color online) **a** Complex modulus ($|G^*_{(\gamma)}|$) as a function of strain amplitude, ranging from 0.01 to 1000% with a fixed frequency of 1 Hz; **b** Complex viscosity ($|\eta^*_{(\omega)}|$); **c** Damping factor ($\tan \delta_{(\omega)}$); **d** Storage modulus ($G'_{(\omega)}$); and **e** loss modulus ($G''_{(\omega)}$) at 200 °C with an amplitude of 5% for the pristine and irradiated PP for various absorbed doses

Fig. 4c. Tan $\delta_{(\omega)}$ is a measure of the damping behavior of polymers[21] which can be correlated with radiation effects [36]. Pristine PP displayed a monotonic reduction in tan $\delta_{(\omega)}$. Irradiated PP showed an increase in tan $\delta_{(\omega)}$ throughout the whole ω range, which exhibited a positive correlation with the absorbed doses. The occurrence of the maximum peak was found for PP irradiated at 200 kGy, corresponding to its reduced elasticity.

Advanced rheological functions were calculated for better quantification, as shown in Fig. 5. First, molecular weight distribution (MMD) plots were made for verifying the linear rheological characteristic of the irradiated PP. MMD spectra were derived from the SAOS tests using the Rheoplus software. As illustrated in Fig. 5a, bimodal molecular weight distributions (MWDs) were found with regard to pristine PP. The peak of the MWD at lower molecular values became sharper and stronger as the absorbed dose increased. The changes at higher molecular values were complex, which may be due to the coexistence of chain scission, branching [37], and cross-linking reactions [38] of the irradiated PP. The reason for this trend will be clarified in our future works.

Cole–Cole plots have been identified as a representative criterion to underline the viscoelastic, viscosity, and elastic responses of polymers [21, 39]. The Cole–Cole plots of the pristine and irradiated PP specimens for various doses are shown in Fig. 5b, in which the imaginary part of $|\eta^*_{(\omega)}|$ (i.e., $\eta''_{(\omega)}$) is plotted versus its real part ($\eta'_{(\omega)}$). All samples displayed a typical arch-like shape. The rising ramp was ascribed to the mainly elastic response, while the descending one was attributed to the viscosity at the lower ω region. As the absorbed dose increased from 45 to 100 kGy, the intensity of the Cole–Cole peaks decreased significantly. We observed that only a reducing ramp was observed for the sample irradiated at 200 kGy, indicating a completely viscous behavior. These results are in good agreement with the work done by Giordano et al. [39], in which they attributed this phenomenon to the degradation of the PP copolymers.

Then, the weighted relaxation spectra, deduced from the SAOS tests, were plotted and are shown in Fig. 5c. These spectra are a useful tool for exploring small molecular processes [37, 40–42]. A bimodal peak at 0.4 s was found for pristine PP, which can be attributed to the PP's segmental relaxation process. It is obvious that the amplitude of this relaxation peak decreased as the absorbed dose increased, implying the facilitated dynamics of the PP segments due to oxidative degradation. More detailed criteria, such as the vGp plot (shown in Fig. 5d) and the plot of $|\eta^*_{(\omega)}|$ versus $|G^*_{(\omega)}|$ (shown in Fig. 5e), were also acquired, which showed similar trends as discussed above.

The mechanical, thermal, and rheological properties of the irradiated PP exhibited great consistence with the structural observations mentioned above. It is evident that the chain scission reactions were predominant when PP was irradiated by 1.2 MeV EBs at low dose rates.

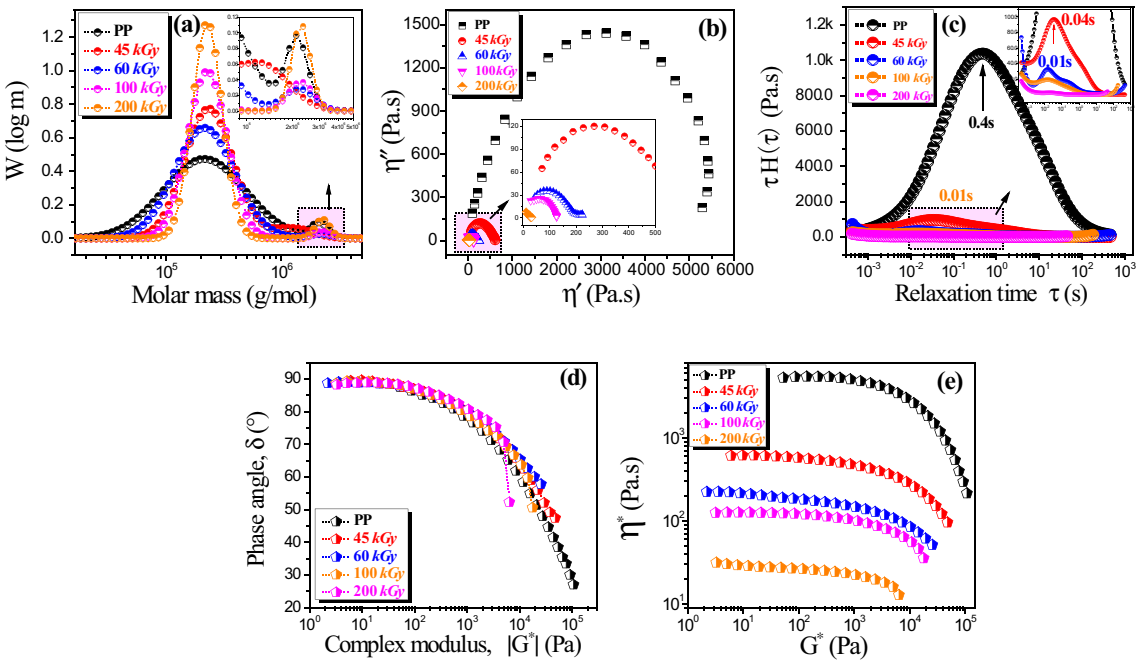

Fig. 5 (Color online) **a** Molecular weight distribution curves, **b** Cole–Cole plots, **c** weighted relaxation spectra, **d** vGp (van Gurp–Palmen) plots, and **e** plot of $|\eta^*_{(\omega)}|$ versus $|G^*_{(\omega)}|$ of the pristine and irradiated PP specimens for various absorbed doses

4 Conclusion

Because information on the EB radiation effects at low dose rates is not available in the literature, it is imperative to understand the EB irradiation effects at low dose rates on PP, from the point of view of the NPP cable industry. This study was carried out mainly to investigate the effects of 1.2 MeV EB irradiation at a static low dose rate of 20 kGy/h, as required by the AP1000 regulation, on the structure and properties of PP and their dependence on the absorbed dose, ranging from 45, to 60, 100, and 200 kGy. The architecture of the irradiated PP was evaluated by interpreting FTIR and ESR measurements, while its properties were estimated from mechanical, thermal, and rheological data. This study leads to the following conclusions. First, we observed that both the CI*s* and C_{Radical} values increased as the absorbed dose increased, implying the gradual increase in oxidative degradation reactions upon irradiation in the presence of oxygen. Secondly, tensile tests showed that the increased absorbed doses, ranging from 45 to 100 kGy, caused deterioration of the mechanical properties, such as reduced tensile strength and elongation at break values, which can be attributed to chain scission reactions of PP upon irradiation. Besides, we found that the overall crystallization behaviors of the irradiated PP changed as a function of the absorbed dose. T_{m}, ΔH_{m}, X_{c}, and T_{c} values decreased as the dose increased, which is indicative of spherulites with a smaller size due to the predominant chain scission reactions. Moreover, our rheological results showed high sensitivity to the structural changes of the irradiated PP; we found that both the $|G^*_{(\gamma)}|$ and $|\eta^*_{(\omega)}|$ values of the irradiated PP significantly decreased as the absorbed dose increased, determined via the amplitude sweeping tests and the SAOS tests, respectively. These phenomena were clarified using advanced rheological functions, such as MWD curves, Cole–Cole plots, and vGp plots. It is clear that the results above indicate a predominant oxidative degradation of PP irradiated by 1.2 MeV EBs at a static low dose rate of 20 kGy.

References

1. K.T. Gillen, M. Celina, R.L. Clough, Density measurements as a condition monitoring approach for following the aging of nuclear power plant cable materials. Radiat. Phys. Chem. **56**, 429–447 (1999). https://doi.org/10.1016/S0969-806X(99)00333-3
2. K.T. Gillen, R.L. Clough, G. Ganouna-Cohen et al., The importance of oxygen in LOCA simulation tests. Nucl. Eng. Des. **74**, 271–285 (1982). https://doi.org/10.1016/0029-5493(83)90065-1
3. J. Wise, K.T. Gillen, M. Celina et al., Time development of diffusion-limited oxidation profiles in a radiation environment. Radiat. Phys. Chem. **49**, 565–573 (1997). https://doi.org/10.1016/S0969-806X(96)00185-5
4. E. Suljovrujic, Post-irradiation effects in polyethylene irradiated under various atmosphere. Radiat. Phys. Chem. **89**, 43–50 (2013). https://doi.org/10.1016/j.radphyschem.2013.04.003
5. B. Katrin, K. Christian, H. Eric et al., The effects of e-beam crosslinking of LDPE on the permeation of hydrocarbons. J. Appl. Polym. Sci. **134**(1–8), 44968 (2017). https://doi.org/10.1002/app.44968/full
6. M.S. Jahan, M.C. King, W.O. Haggard et al., A study of long-lived radicals in gamma-irradiated medical grade polyethylene. Radiat. Phys. Chem. **62**, 141–144 (2001). https://doi.org/10.1016/S0969-806X(01)00431-5
7. S. Dadbin, M. Frounchi, M.H. Saeid et al., Molecular structure and physical properties of e-beam crosslinked low-density polyethylene for wire and cable insulation applications. J. Appl. Polym. Sci. **86**, 1959–1969 (2002). https://doi.org/10.1002/app.11111/full
8. H.R. Víctor, K. Matthias, H.W. Manfred, Size exclusion chromatography of photo-oxidated LDPE by triple detection and its relation to rheological behavior. Polym. Degrad. Stab. **111**, 46–54 (2015). https://doi.org/10.1016/j.polymdegradstab.2014.10.022
9. E. Mehdi, A. Mahdi, A. Mostafa, Theoretical correlation of linear and non-linear rheological symptoms of long-chain branching in polyethylene irradiated by electron beam at relatively low doses. Rheo. Acta. **56**, 729–742 (2017). https://doi.org/10.1007/s00397-017-1029-9
10. A.E. Goulas, K.A. Riganakos, M.G. Kontominas, Effect of ionizing radiation on physicochemical and mechanical properties of commercial monolayer and multilayer semirigid plastic materials. Radiat. Phys. Chem. **69**, 411–417 (2004). https://doi.org/10.1016/j.radphyschem.2003.08.013
11. M.A. Lopez, G. Burillo, A. Charlesby, Studies on memory effect in polyethylene. Radiat. Phys. Chem. **43**, 227–231 (1994). https://doi.org/10.1016/0969-806X(94)90183-X
12. K. Damir, Š. Mario, B. Goran et al., Influence of high doses γ-irradiation on oxygen permeability of linear low-density polyethylene and cast polypropylene films. Radiat. Phys. Chem. **97**, 304–312 (2014). https://doi.org/10.1016/j.radphyschem.2013.12.005
13. R.P. Joshi, K. Hareesh, A. Bankar et al., Anti-biofilm efficacy of 100 MeV gold ion irradiated polycarbonate against salmonella typhi. Radiat. Phys. Chem. **141**, 149–154 (2017). https://doi.org/10.1016/j.radphyschem.2017.07.002
14. P. Dahal, Y.C. Kim, Preparation and characterization of modified polypropylene by using electron beam irradiation. J. Ind. Eng. Chem. **19**, 1879–1883 (2013). https://doi.org/10.1016/j.jiec.2013.02.027
15. D. Auhl, J. Stange, H. Münstedt et al., Long-chain branched polypropylenes by electron beam irradiation and their rheological properties. Macromolecules **37**, 9465–9472 (2004). https://doi.org/10.1021/ma030579w
16. D. Wan, L. Ma, H.P. Xing et al., Preparation and characterization of long chain branched polypropylene mediated by different heteroaromatic ring derivatives. Polymer **54**, 639–651 (2013). https://doi.org/10.1016/j.polymer.2012.12.014
17. J. Guapacha, M.D. Failla, E.M. Vallés et al., Molecular, rheological, and thermal study of long-chain branched polypropylene obtained by esterification of anhydride grafted polypropylene. J. Appl. Polym. Sci. **131**, 40357 (2014). https://doi.org/10.1002/app.40357/full
18. H. Otaguro, L.F.C.P. Lima, D.F. Parra et al., High-energy radiation forming chain scission and branching in polypropylene. Radiat. Phys. Chem. **79**, 318–324 (2010). https://doi.org/10.1016/j.radphyschem.2009.11.003
19. A.T. Fintzou, M.G. Kontominas, A.V. Badeka et al., Effect of electron-beam and gamma-irradiation on physicochemical and mechanical properties of polypropylene syringes as a function of

irradiation dose: Study under vacuum. Radiat. Phys. Chem. **76**, 1147–1155 (2007). https://doi.org/10.1016/j.radphyschem.2006.11.009
20. B. Bartoníček, V. Plaček, V. Hnát, Comparison of degradation effects induced by gamma radiation and electron beam radiation in two cable jacketing materials. Radiat. Phys. Chem. **76**, 857–863 (2007). https://doi.org/10.1016/j.radphyschem.2006.05.011
21. A.C. Abraham, M.A. Czayka, M.R. Fisch, Electron beam irradiations of polypropylene syring barrels and the resulting ohysical and chemical property changes. Radiat. Phys. Chem. **79**, 83–92 (2010). https://doi.org/10.1016/j.radphyschem.2009.08.027
22. F. Ardakani, Y. Jahani, J. Morshedian, The role of PB-1 on the long chain branching of PP by electron beam irradiation in solid state and melt viscoelastic behavior. Radiat. Phys. Chem. **87**, 64–70 (2013). https://doi.org/10.1016/j.radphyschem.2013.02.021
23. R. Tobias, M. Dieter, F. Christian et al., Determination of the relaxation time spectrum from dynamic moduli using an edge preserving regulation method. Rheol. Acta **39**, 163–173 (2000). https://doi.org/10.1007/s003970050016
24. C. Lang, A Laplace transform method for molecular mass distribution calculation from rheometric data. J. Rheol. **61**, 947–954 (2017). https://doi.org/10.1122/1.4995602
25. J. Reuben, B.H. Mahlman, The fate of peroxy radicals in irradiated polypropylene. An ESR investigation with oxygen-17 labeling. J. Phys. Chem. **88**, 4904–4906 (1984). https://doi.org/10.1021/j150665a021
26. D.M. Mowery, R.A. Assink, D.K. Derzon et al., Solid-state ^{13}C NMR investigation of the oxidative degradation of selectively labeled polypropylene by thermal aging and gamma-irradiation. Macromolecules **28**, 5035–5046 (2005). https://doi.org/10.1021/ma047381b
27. U.A. Sevil, O. Güven, Spectroscopic, viscometric and mechanical characterization of γ-irradiated isotactic polypropylene syringes. Radiat. Phys. Chem. **46**, 875–878 (1995). https://doi.org/10.1016/0969-806X(95)00282-3
28. G. Khang, J.M. Rhee, J.K. Jeong et al., Local drug delivery system using biodegradable polymers. Macromol. Res. **11**, 207–223 (2003). https://doi.org/10.1007/BF03218355
29. A.T. Fintzou, A.V. Badeka, M.G. Kontominas et al., Changes in physicochemical properties of γ-irradiated polypropylene syringes as a function of irradiation dose. Radiat. Phys. Chem. **75**, 87–97 (2006). https://doi.org/10.1016/j.radphyschem.2005.03.014
30. T. Sawaguchi, T. Ikemura, M. Seno, Preparation of alpha., omega.-Diisopropenyloligopropylene by thermal degradation of isotactic polypropylene. Macromolecules **28**, 7973–7978 (1995). https://doi.org/10.1021/ma00128a001
31. K.A. Riganakos, W.D. Koller, D.A.E. Ehlermann et al., Effects of ionizing radiation on properties of manolayer and multilayer flexible food packaging materials. Radiat. Phys. Chem. **54**, 527–540 (1999). https://doi.org/10.1016/S0969-806X(98)00263-1
32. S. Chytiri, A.E. Goulas, K.A. Riganakos et al., Thermal, mechanical and permeation properties of gamma-irradiated multilayer food packaging films containing a buried layer of recycled low density polyethylene. Radiat. Phys. Chem. **75**, 416–423 (2006). https://doi.org/10.1016/j.radphyschem.2005.07.005
33. I. Krupa, A.S. Luyt, Thermal properties of isotactic propylene degraded with gamma radiation. Polym. Degrad. Stab. **72**, 505–508 (2001). https://doi.org/10.1016/S0141-3910(01)00052-0
34. N. Yagoubi, R. Peron, B. Legendre et al., Gamma and electron beam radiation induced physico-chemical modification of poly (propylene). Nucl. Instract. Method B **151**, 247–254 (1999). https://doi.org/10.1016/S0168-583X(99)00157-3
35. X.C. Zhang, M.F. Butler, R.E. Cameron, The ductile-brittle transition of irradiated isotactic polypropylene studied using simultaneous small angle X-ray scattering and tensile deformation. Polymer **41**, 3797–3807 (2010). https://doi.org/10.1016/S0032-3861(99)00594-7
36. S.A. Mousavi, S. Dadbin, M. Frounchi et al., Comparison of rheological behavior of branched polypropylene prepared by chemical modification and electron beam irradiation under air and N_2. Radiat. Phys. Chem. **79**, 1008–1094 (2010). https://doi.org/10.1016/j.radphyschem.2010.04.010
37. W.L. Oliani, D.F. Parra, D.M. Fermino et al., Study of gel formation by ionizing radiation in polypropylene. Radiat. Phys. Chem. **84**, 20–25 (2013). https://doi.org/10.1016/j.radphyschem.2012.06.053
38. A.J. Satti, J.A. Ressia, M.L. Cerrada et al., Rheological analysis of irradiated crosslinkable and scissionable polymers used for medical devices under different radiation conditions. Radiat. Phys. Chem. **144**, 298–303 (2018). https://doi.org/10.1016/j.radphyschem.2017.09.002
39. F. Zulli, L. Andreozzi, E. Passaglia et al., Rheology of long-chain branched polypropylene copolymers. J. Appl. Poly. Sci. **127**, 1423–1432 (2013). https://doi.org/10.1002/app.38076/full
40. B. Leila, K. Alireza, A.B. Mohammad et al., Correlation between viscoelastic behavior and morphology of nanocomposites based on SR/EPDM blends compatibilized by maleic anhydride. Polymer **113**, 156–166 (2017). https://doi.org/10.1016/j.polymer.2017.02.057
41. H. Víctor, G. Rolón, H.W. Manfred, Linear and non-linear rheological characterization of photo-oxidative degraded LDPE. Polym. Degrad. Stab. **99**, 136–145 (2014). https://doi.org/10.1016/j.polymdegradstab.2013.11.014
42. A.K. Murray, J.E. Kennedy, B. McEvoy et al., The effect of high energy electron beam irradiation in air on accelerated aging and on the structure property relationships of low density polyethylene. Nucl. Instrum. Methods B **297**, 64–74 (2013). https://doi.org/10.1016/j.nimb.2012.12.001